

LENGTH PRESERVING NUMERICAL SCHEMES FOR LANDAU-LIFSHITZ EQUATION BASED ON LAGRANGE MULTIPLIER APPROACHES

QING CHENG* AND JIE SHEN†

Abstract. We develop in this paper two classes of length preserving schemes for the Landau-Lifshitz equation based on two different Lagrange multiplier approaches. In the first approach, the Lagrange multiplier $\lambda(\mathbf{x}, t)$ equals to $|\nabla m(\mathbf{x}, t)|^2$ at the continuous level, while in the second approach, the Lagrange multiplier $\lambda(\mathbf{x}, t)$ is introduced to enforce the length constraint at the discrete level and is identically zero at the continuous level. By using a predictor-corrector approach, we construct efficient and robust length preserving higher-order schemes for the Landau-Lifshitz equation, with the computational cost dominated by the predictor step which is simply a semi-implicit scheme. Furthermore, by introducing another space-independent Lagrange multiplier, we construct energy dissipative, in addition to length preserving, schemes for the Landau-Lifshitz equation, at the expense of solving one nonlinear algebraic equation. We present ample numerical experiments to validate the stability and accuracy for the proposed schemes, and also provide a performance comparison with some existing schemes.

Key words. Landau-Lifshitz equation; Lagrange multiplier, energy stability, projection method

AMS subject classifications. 65M70; 65N22; 65N12; 35K61

1. Introduction. We consider the Landau-Lifshitz equation (with $\beta \neq 0$, it is often referred as the Landau-Lifshitz-Gilbert equation) in the following form [18, 33]:

$$(1.1) \quad \begin{aligned} m_t &= -\beta m \times \Delta m - \gamma m \times (m \times \Delta m) \quad \text{in } \Omega, \\ m(\mathbf{x}, 0) &= m_0(\mathbf{x}), \end{aligned}$$

with either homogeneous Neumann or periodic boundary condition. In the above, the unknown $m = (m_1, m_2, m_3)^t$ describes the magnetization in continuum ferromagnets, Ω is an open bounded domain in R^d ($d = 1, 2, 3$), β is an exchange parameter, $\gamma > 0$ is the Gilbert damping parameter, and $m_0(\mathbf{x})$ with $|m_0(\mathbf{x})| \equiv 1$ is the initial condition. An important property of (1.1) is that the solution m preserves pointwisely its magnitude. Indeed, taking the dot product of (1.1) with m , we derive that vector field m satisfies $\frac{d}{dt}|m(\mathbf{x})| = 0$ for all $\mathbf{x} \in \Omega$, so that solutions of (1.1) satisfy an implicit constraint

$$(1.2) \quad |m(\mathbf{x}, t)| = 1 \quad \forall \mathbf{x} \in \Omega,$$

i.e., m is length preserving. Another important property is that (1.1) obeys an energy dissipation law. Taking the inner product of the first equation in (1.1) with Δm , we find that (1.1) satisfies the following energy dissipative law

$$(1.3) \quad \frac{d}{dt} \int_{\Omega} \frac{1}{2} |\nabla m|^2 d\mathbf{x} = -\gamma \|m \times \Delta m\|^2.$$

The Landau-Lifshitz equation (1.1), derived in [21] to describe the evolution of magnetization, plays a very important role in understanding of non-equilibrium magnetism, and its accurate numerical simulation has become an effective tool in understanding both the static and dynamics in ferromagnetic materials [19, 20]. Much effort has been developed in the past several decades to develop efficient and accurate numerical methods for solving the Landau-Lifshitz equation [17, 4, 5, 15].

To construct accurate and stable numerical schemes for the Landau-Lifshitz equation, it is of critical importance to ensure that the key physical constraint $|m| = 1$ is preserved at the discrete

*Department of Mathematics, Purdue University West Lafayette, IN 47907, USA (cheng573@purdue.edu).

†Department of Mathematics, Purdue University, West Lafayette, IN 47907, USA (shen7@purdue.edu). The work of J.S. is supported in part by NSF DMS-1720442 and NFSC 11971407.

level. Existing numerical schemes for enforcing the length constraint $|m| = 1$ can be roughly classified into two categories: (i) Penalty approach [26, 27]: adding a penalty term to approximate the constraint $|m| = 1$. The penalty approach has been frequently used in numerical approximation of liquid crystal flows [7, 6, 24, 25], but introduces additional numerical difficulties associated with the penalty parameters and does not enforce the length constraint exactly. (ii) Projection approach [33, 8, 4]: in the first-step, finding a approximate solution without enforcing the constraint, then performing a simple projection in the second step to enforce the constraint. Due to the simplicity of the projection approach, it has been frequently used, see, for instance. [33, 32, 3, 4]. Recently, a L^2 -average orthogonal projection method is proposed in [2] where the length constraint is enforced in the sense of L^2 -average. On the other hand, it appears to be difficult to construct higher-order robust schemes based on the projection approach. Furthermore, as our analysis indicates, the schemes based on the projection approach can not satisfy a discrete energy dissipation law.

In a sequence of recent work [12, 13], we proposed efficient positivity/bound preserving schemes based on the Lagrange multiplier approach for a class of complex nonlinear systems. The main purpose of this paper is to construct efficient length preserving schemes based on the Lagrange multiplier approach for the Landau-Lifshitz equation. More precisely, we introduce a new Lagrange multiplier approach, which at its simplest form reduces to the simple projection approach proposed in [33], and couple it with a predictor-corrector approach to construct efficient and robust length preserving higher-order schemes for the Landau-Lifshitz equation. Furthermore, by introducing another space-independent Lagrange multiplier, we can also construct energy dissipative, in addition to length preserving, schemes for the Landau-Lifshitz equation, at the expense of solving one nonlinear algebraic equation. To the best of our knowledge, our schemes based on the predictor-corrector approach are the first length preserving higher than second-order schemes for the Landau-Lifshitz equation, and our schemes with an additional space-independent Lagrange multiplier are the first length preserving and energy dissipative schemes for the Landau-Lifshitz equation.

The paper is organized as follows. In Section 2, we present two different formulations of the Landau-Lifshitz equation (for both the special case with $\beta = 0$ and the general case with $\beta \neq 0$) by introducing a Lagrange multiplier to enforce the length constraints. In Section 3, we construct a class of robust and accurate length preserving schemes for the special Landau-Lifshitz equation with $\beta = 0$ based on the operator splitting and predictor-corrector approach. In Section 4, we modify the length preserving schemes in Section 3 so that they also dissipate the energy. We then construct length preserving schemes and length preserving/energy decreasing schemes for the general Landau-Lifshitz equation in Section 5. In Section 6, we present ample numerical experiments to validate the stability and accuracy for the proposed schemes and provide a performance comparison with some existing schemes. We conclude with some remarks in the final section.

2. Formulations of Landau-Lifshitz equation with Lagrange multipliers. It is pointed out in [33] that descretizing directly (2.1) without enforcing $|m| = 1$ will lead to unstable numerical solutions. Hence, we shall consider expanded formulation of (2.1) by introducing a Lagrange multiplier to enforce the length constraint.

Since it is difficult to deal with $-m \times (m \times \Delta m)$ implicitly in a numerical scheme while an explicit treatment will lead to a severe time step constraint, we first rewrite (1.1) as

$$(2.1) \quad m_t = -\beta m \times \Delta m + \gamma(\Delta m + |\nabla m|^2 m).$$

In the above, we used the fact that $-m \times (m \times \Delta m) = \Delta m + |\nabla m|^2 m$ if $|m| = 1$, which can be derived from the identity

$$(2.2) \quad a \times (b \times c) = (a \cdot c)b - (a \cdot b)c, \quad a, b, c \in \mathbb{R}^3.$$

Then, we introduce a Lagrange multiplier $\lambda(\mathbf{x}, t)$ to enforce the length constraint and consider:

$$(2.3) \quad \begin{aligned} m_t &= -\beta m \times \Delta m + \gamma(\Delta m + |\nabla m|^2 m) + \lambda(\mathbf{x}, t)m, \\ |m(\mathbf{x}, t)| &= 1. \end{aligned}$$

Obviously with $\lambda(\mathbf{x}, t) \equiv 0$, the above system is equivalent to (2.1). But we can now discretize (2.3) directly with $|m(\mathbf{x}, t)| = 1$ explicitly enforced.

We shall also consider an alternative formulation using a Lagrange multiplier as in [33]. Using the identity

$$(2.4) \quad \frac{1}{2} \Delta |m|^2 = m \cdot \Delta m + |\nabla m|^2,$$

we find that

$$(2.5) \quad -m \cdot \Delta m = |\nabla m|^2 \quad \text{if } |m(x)| = 1.$$

Hence, we can rewrite (2.1) with $|m| = 1$ in the following equivalent form:

$$(2.6) \quad \begin{aligned} m_t &= -\beta m \times \Delta m + \gamma(\Delta m + \lambda(\mathbf{x}, t)m), \\ |m(\mathbf{x}, t)| &= 1. \end{aligned}$$

Indeed, multiplying the above by m and using (2.5) and the fact that $|m(\mathbf{x}, t)| = 1$, we find that $\lambda = |\nabla m|^2$. Hence, λ can also be viewed as the Lagrange multiplier for the constraint $|m(\mathbf{x}, t)| = 1$.

A case of particular interest is when $\beta = 0$. For the sake of simplicity, we also set $\gamma = 1$. In this case, (2.1) becomes

$$(2.7) \quad m_t = \Delta m + |\nabla m|^2 m;$$

while (2.3) becomes

$$(2.8) \quad \begin{aligned} m_t &= \Delta m + |\nabla m|^2 m + \lambda(\mathbf{x}, t)m, \\ |m(\mathbf{x}, t)| &= 1; \end{aligned}$$

and (2.6) becomes

$$(2.9) \quad \begin{aligned} m_t &= \Delta m + \lambda(\mathbf{x}, t)m, \\ |m(\mathbf{x}, t)| &= 1. \end{aligned}$$

The equation (2.8) or (2.9) is also called the heat flow for harmonic maps, and has been extensively studied mathematically and numerically [17, 10, 23].

In the next section, we shall develop several numerical schemes for this special case based on both (2.8) and (2.9). Extensions to the more general cases based on (2.3) and (2.6) will be considered in Section 5. In the following, we shall refer to schemes based on (2.9) and (2.6) as Type-I schemes, and those based on (2.8) and (2.3) as Type-II schemes. Since the constructions of the Type-I and Type-II schemes follow essentially the same procedure, we shall present the Type-I schemes for with sufficient details and explain briefly how to construct Type-II schemes.

3. Length preserving time discretization schemes for the special Landau-Lifshitz equation (2.7). In this section, we construct a class of efficient schemes for (2.9) and (2.8). Note that $\lambda(\mathbf{x}, t)$ (resp. $|m(\mathbf{x}, t)| = 1$) in (2.9) and (2.8) plays a role similar to the pressure (resp. incompressibility constraint) in the Navier-Stokes equations. Hence, we can adopt the operator splitting and pressure-correction approaches developed for the Navier-Stokes equations for solving (2.9) and (2.8).

3.1. Type-I first-order operator-splitting scheme. Similarly to the Chorin-Temam projection method for the Navier-Stokes equations [14, 31], we introduce a first-order operator-splitting scheme for Landau-Lifshitz equation (2.9). Assuming $m^n = (m_1^n, m_2^n, m_3^n)$ is known, we solve \tilde{m}^{n+1} from

$$(3.1) \quad \frac{\tilde{m}^{n+1} - m^n}{\delta t} = \Delta \tilde{m}^{n+1},$$

and then we solve λ^{n+1}, m^{n+1} from

$$(3.2) \quad \frac{m^{n+1} - \tilde{m}^{n+1}}{\delta t} = \lambda^{n+1} m^{n+1},$$

$$(3.3) \quad |m^{n+1}| = 1.$$

THEOREM 3.1. *The scheme (3.2)-(3.3) admits two sets of solution, and the set of solution consistent to (2.9) is given by*

$$(3.4) \quad \lambda^{n+1} = \frac{1 - |\tilde{m}^{n+1}|}{\delta t}, \quad m^{n+1} = \frac{\tilde{m}^{n+1}}{|\tilde{m}^{n+1}|}.$$

Proof. We rewrite (3.2) as

$$(3.5) \quad (1 - \delta t \lambda^{n+1}) m^{n+1} = \tilde{m}^{n+1}.$$

Multiplying (3.5) with itself on both sides, thanks to $|m^{n+1}| = 1$, we derive

$$(3.6) \quad (1 - \delta t \lambda^{n+1})^2 = |\tilde{m}^{n+1}|^2.$$

There are two roots for the above equation

$$(3.7) \quad \lambda^{n+1} = \frac{1 - |\tilde{m}^{n+1}|}{\delta t} \quad \text{or} \quad \lambda^{n+1} = \frac{1 + |\tilde{m}^{n+1}|}{\delta t}.$$

Below we show that $\lambda^{n+1} = \frac{1 - |\tilde{m}^{n+1}|}{\delta t}$ is the only right solution.

We derive from (3.1) that $\tilde{m}^{n+1} = (I - \delta t \Delta)^{-1} m^n \approx m^n + \delta t \Delta m^n$. Hence,

$$(3.8) \quad |\tilde{m}^{n+1}|^2 \approx 1 + 2\delta t m^n \cdot \Delta m^n + \delta t^2 \delta t (m^n \cdot \Delta m^n)^2 \approx (1 + \delta t m^n \cdot \Delta m^n)^2 \approx (1 - \delta t |\nabla m^n|^2)^2,$$

where we used equality (2.5).

Using the above equation, we derive

$$\lambda^{n+1} = \frac{1 - |\tilde{m}^{n+1}|}{\delta t} \approx \frac{1 - (1 - \delta t |\nabla m^n|^2)}{\delta t} \approx |\nabla m^n|^2,$$

which is consistent with $\lambda(x, t) = -m(x, t) \cdot \Delta m(x, t) = |\nabla m|^2$ at the continuous level. Plugging $\lambda^{n+1} = \frac{1 - |\tilde{m}^{n+1}|}{\delta t}$ into equation (3.2), we obtain $m^{n+1} = \frac{\tilde{m}^{n+1}}{|\tilde{m}^{n+1}|}$. \square

The above result indicates that the scheme (3.1)-(3.3) is equivalent to the projection scheme in [33]. Hence, (3.1)-(3.3) is an alternative formulation of the projection scheme, and it opens up a new avenue to develop higher-order version.

We recall that a stability and error analysis in L^∞ -norm for the projection scheme was carried out in [33]. Below, we provide an alternative stability analysis in L^2 -norm for the scheme (3.1)-(3.3).

We first recall the following result from [33].

LEMMA 3.1. Assume that

$$(3.9) \quad (I - \alpha \delta t \Delta) m = f \quad \text{in } \Omega$$

with the homogeneous Neumann boundary condition or periodic boundary condition where $m = (m_1, m_2, m_3)$, $f = (f_1, f_2, f_3)$ and α is any positive constant. Then

$$(3.10) \quad \max_{\forall x} |m| \leq \max_{\forall x} |f|.$$

LEMMA 3.2. If the exact solution m of Landau-Lifshitz equations poss enough regularity, for Lagrange multiplier λ^{n+1} , we have the following bound

$$(3.11) \quad 0 \leq \lambda^{n+1}(\mathbf{x}) \leq C_0,$$

for any \mathbf{x} in the domain Ω , where C_0 is a constant independent of δt .

Proof. Since $|m^n| = 1$, we derive immediately from (3.1) and Lemma 3.1 that

$$(3.12) \quad |\tilde{m}^{n+1}| \leq 1.$$

Then we derive from the above and (3.4) that $\lambda^{n+1} \geq 0$. It is shown in (3.33) of [33] that there exists $C_0 > 0$ such that

$$|\tilde{m}^{n+1}| \geq 1 - C_0 \delta t,$$

which, together with (3.4), implies that $\lambda^{n+1}(\mathbf{x}) \leq C_0$. □

We are now in position to prove the following stability results.

THEOREM 3.3. For the scheme (3.1)-(3.3), we have

$$(3.13) \quad \|\nabla m^k\|^2 + 2\delta t \sum_{n=0}^{k-1} (\|\nabla \tilde{m}^{n+1} - \nabla m^n\|^2 + \|\nabla m^{n+1} - \nabla \tilde{m}^{n+1}\|^2) \leq \tilde{C} \|\nabla m^0\|^2,$$

where \tilde{C} is a positive constant depending on C_0 and T .

Proof. Taking the inner product of equation (3.1) with $-\frac{\tilde{m}^{n+1} - m^n}{\delta t}$, we obtain

$$(3.14) \quad -\left\| \frac{\tilde{m}^{n+1} - m^n}{\delta t} \right\|^2 = \frac{1}{2\delta t} (\|\nabla \tilde{m}^{n+1}\|^2 - \|\nabla m^n\|^2 + \|\nabla \tilde{m}^{n+1} - \nabla m^n\|^2).$$

Taking the inner product of equation (3.2) with $-\Delta m^{n+1}$, we obtain

$$(3.15) \quad \frac{1}{2\delta t} (\|\nabla m^{n+1}\|^2 - \|\nabla \tilde{m}^{n+1}\|^2 + \|\nabla m^{n+1} - \nabla \tilde{m}^{n+1}\|^2) = -(\lambda^{n+1} m^{n+1}, \Delta m^{n+1}).$$

Summing up equation (3.14) and equation (3.15), we obtain

$$(3.16) \quad \begin{aligned} & -\left\| \frac{\tilde{m}^{n+1} - m^n}{\delta t} \right\|^2 - (\lambda^{n+1} m^{n+1}, \Delta m^{n+1}) \\ & = \frac{1}{2\delta t} (\|\nabla m^{n+1}\|^2 - \|\nabla m^n\|^2 + \|\nabla \tilde{m}^{n+1} - \nabla m^n\|^2 + \|\nabla m^{n+1} - \nabla \tilde{m}^{n+1}\|^2). \end{aligned}$$

Since $|m^{n+1}| = 1$, we have $m^{n+1} \Delta m^{n+1} + |\nabla m^{n+1}|^2 = 0$, which implies

$$(3.17) \quad -(\lambda^{n+1} m^{n+1}, \Delta m^{n+1}) = (\lambda^{n+1}, |\nabla m^{n+1}|^2).$$

We can then rewrite (3.16) as

$$(3.18) \quad -\left\|\frac{\tilde{m}^{n+1} - m^n}{\delta t}\right\|^2 = \frac{1}{2\delta t}(\|\nabla m^{n+1}\|^2 - \|\nabla m^n\|^2 + \|\nabla \tilde{m}^{n+1} - \nabla m^n\|^2 + \|\nabla m^{n+1} - \nabla \tilde{m}^{n+1}\|^2) - (\lambda^{n+1}, |\nabla m^{n+1}|^2).$$

By Lemma 3.2, we have $0 \leq \lambda^{n+1} \leq C_0$. Summing up equation (3.18) for $n = 1, 2, \dots, k-1 = \frac{T}{\delta t} - 1$, we obtain

$$(3.19) \quad \begin{aligned} & \|\nabla m^k\|^2 + 2\delta t \sum_{n=0}^{k-1} (\|\nabla \tilde{m}^{n+1} - \nabla m^n\|^2 + \|\nabla m^{n+1} - \nabla \tilde{m}^{n+1}\|^2) \\ & \leq \|\nabla m^0\|^2 + 2\delta t C_0 \sum_{n=0}^{k-1} \|\nabla m^{n+1}\|^2. \end{aligned}$$

Applying a discrete Gronwall Lemma (cf. Lemma 2 in [28]) to the above, we obtain

$$(3.20) \quad \|\nabla m^k\|^2 + 2\delta t \sum_{n=0}^{k-1} (\|\nabla \tilde{m}^{n+1} - \nabla m^n\|^2 + \|\nabla m^{n+1} - \nabla \tilde{m}^{n+1}\|^2) \leq \tilde{C} \|\nabla m^0\|^2. \quad \square$$

3.2. Type-I higher-order predictor-corrector schemes. Theorem 3.1 shows that the first-order operator splitting scheme (3.1)-(3.3) is equivalent to the projection scheme introduced in [33]. Hence, it provides an alternative interpretation of the projection scheme. More importantly, it opens up a new avenue to develop higher-order schemes for (2.8) through a predictor-corrector approach as we show below. Note that it is difficult to construct higher-order schemes based on the projection scheme, see [33] for an attempt on constructing a second-order scheme. However, using an idea similar to the pressure-correction scheme for the Navier-Stokes equations (see, for instance, [16]), we can construct higher-order schemes for (2.9) through a predictor-corrector approach as follows.

Step 1 (Predictor): solve \tilde{m}^{n+1} from

$$(3.21) \quad \frac{\alpha_k \tilde{m}^{n+1} - A_k(m^n)}{\delta t} = \Delta \tilde{m}^{n+1} + B_{k-1}(\lambda^n m^n),$$

Step 2 (Corrector): solve (m^{n+1}, λ^{n+1}) from

$$(3.22) \quad \frac{\alpha_k(m^{n+1} - \tilde{m}^{n+1})}{\delta t} = \lambda^{n+1} m^{n+1} - B_{k-1}(\lambda^n m^n),$$

$$(3.23) \quad |m^{n+1}| = 1,$$

where α_k , and A_k are determined from the k th-order Backward Difference-Formulas (BDF) [1, 12, 13], and B_{k-1} is determined from the Adams-Bashforth extrapolation:

First-order:

$$(3.24) \quad \alpha_1 = 1, \quad A_1(m^n) = m^n, \quad B_0(\lambda^n m^n) = 0;$$

Second-order:

$$(3.25) \quad \alpha_2 = \frac{3}{2}, \quad A_2(m^n) = 2m^n - \frac{1}{2}m^{n-1}, \quad B_1(\lambda^n m^n) = \lambda^n m^n;$$

Third-order:

$$(3.26) \quad \alpha_3 = \frac{11}{6}, \quad A_3(m^n) = 3m^n - \frac{3}{2}m^{n-1} + \frac{1}{3}m^{n-2}, \quad B_2(\lambda^n m^n) = 2\lambda^n m^n - \lambda^{n-1}m^{n-1}.$$

The formula for $k = 4, 5, 6$ can be derived similarly with Taylor expansions.

We observe that the first step is a usual k th-order Implicit-Explicit (IMEX) scheme for the first equation in (2.9), while the second step is k th-order correction to enforce $|m| = 1$. Obviously, \tilde{m}^{n+1} can be easily obtained from the first step. Below we show how to efficiently solve (m^{n+1}, λ^{n+1}) in the second step. We rewrite (3.22) into the equivalent form

$$(3.27) \quad \frac{\alpha_k \left(m^{n+1} - \left(\tilde{m}^{n+1} - \frac{\delta t}{\alpha_k} B_{k-1}(\lambda^n m^n) \right) \right)}{\delta t} = \lambda^{n+1} m^{n+1},$$

and rearrange it into

$$(3.28) \quad (\alpha_k - \delta t \lambda^{n+1}) m^{n+1} = \alpha_k \tilde{m}^{n+1} - \delta t B_{k-1}(\lambda^n m^n).$$

Multiplying (3.28) with itself on both sides and using (3.23), we obtain

$$(3.29) \quad (\alpha_k - \delta t \lambda^{n+1})^2 = |\alpha_k \tilde{m}^{n+1} - \delta t B_{k-1}(\lambda^n m^n)|^2.$$

Then, similarly to the proof of Theorem 3.1, we can establish the following result:

THEOREM 3.2. *The scheme (3.21)-(3.23) admits two sets of solution, and the set of solution consistent to (2.9) is given by*

$$(3.30) \quad \lambda^{n+1} = \frac{\alpha_k - |\alpha_k \tilde{m}^{n+1} - \delta t B_{k-1}(\lambda^n m^n)|}{\delta t},$$

and

$$(3.31) \quad m^{n+1} = \frac{\alpha_k \tilde{m}^{n+1} - \delta t B_{k-1}(\lambda^n m^n)}{|\alpha_k \tilde{m}^{n+1} - \delta t B_{k-1}(\lambda^n m^n)|}.$$

In summary, the scheme (3.21)-(3.23) can be implemented as follows:

- Solve \tilde{m}^{n+1} from (3.21);
- Find m^{n+1} from projection step (3.31);
- Update λ^{n+1} by (3.30).

Remark 3.1. *We observe from (3.31) that the scheme (3.21)-(3.23) can be viewed as a modified projection method:*

Step 1 (Predictor): solve \tilde{m}^{n+1} from

$$(3.32) \quad \frac{\alpha_k \tilde{m}^{n+1} - A_k(m^n)}{\delta t} = \Delta \tilde{m}^{n+1} + B_{k-1}(\lambda^n m^n),$$

Step 2 (Projection): solve m^{n+1} from

$$(3.33) \quad m^{n+1} = \frac{\alpha_k \tilde{m}^{n+1} - \delta t B_{k-1}(\lambda^n m^n)}{|\alpha_k \tilde{m}^{n+1} - \delta t B_{k-1}(\lambda^n m^n)|},$$

and update the Lagrange multiplier $\lambda^{n+1} = \frac{\alpha_k - |\alpha_k \tilde{m}^{n+1} - \delta t B_{k-1}(\lambda^n m^n)|}{\delta t}$.

Remark 3.2. *We emphasize that one can construct other higher-order schemes using the predictor-corrector approach. For example, a second-order scheme based on Crank-Nicolson is as follows: Find \tilde{m}^{n+1} from*

$$(3.34) \quad \frac{\tilde{m}^{n+1} - m^n}{\delta t} = \Delta \frac{\tilde{m}^{n+1} + \tilde{m}^n}{2} + \lambda^n m^n;$$

and find λ^{n+1} , m^{n+1} from

$$(3.35) \quad \frac{m^{n+1} - \tilde{m}^{n+1}}{\delta t} = \frac{\lambda^{n+1} m^{n+1} - \lambda^n m^n}{2},$$

$$(3.36) \quad |m^{n+1}| = 1.$$

It is easy to see that (3.35)-(3.36) can be solved similarly as (3.22)-(3.23).

Remark 3.3. The key to prove the uniform bound in Theorem 3.3 is the bound for λ in Lemma 3.2. On the other hand, we also observe from the bound (3.11) and (3.18) that the scheme can not be energy dissipative.

It appears difficult to establish similar bound as (3.11) for the above higher-order schemes, consequently, proving a uniform bound as in Theorem 3.3 is also illusive.

3.3. Type-II length preserving schemes. Similarly to (3.21)-(3.23), we can construct higher-order predictor-corrector schemes for (2.8) as follows.

Step 1 (Predictor): solve \tilde{m}^{n+1} from

$$(3.37) \quad \frac{\alpha_k \tilde{m}^{n+1} - A_k(m^n)}{\delta t} = \Delta \tilde{m}^{n+1} + B_k(|\nabla m^n|^2 m^n) + B_{k-1}(\lambda^n m^n),$$

Step 2 (Corrector): solve (m^{n+1}, λ^{n+1}) from

$$(3.38) \quad \frac{\alpha_k(m^{n+1} - \tilde{m}^{n+1})}{\delta t} = \lambda^{n+1} m^{n+1} - B_{k-1}(\lambda^n m^n),$$

$$(3.39) \quad |m^{n+1}| = 1,$$

where α_k , the operators A_k and B_{k-1} ($k = 1, 2, 3$) are given by (3.24)-(3.26).

Similarly to (3.22)-(3.23), we can show that the above scheme admits two sets of solution and the one which is consistent to (2.8) is given by:

$$(3.40) \quad \begin{aligned} \lambda^{n+1} &= \frac{\alpha_k - |\alpha_k \tilde{m}^{n+1} - \delta t B_{k-1}(\lambda^n m^n)|}{\delta t}, \\ m^{n+1} &= \frac{\alpha_k \tilde{m}^{n+1} - \delta t B_{k-1}(\lambda^n m^n)}{|\alpha_k \tilde{m}^{n+1} - \delta t B_{k-1}(\lambda^n m^n)|}. \end{aligned}$$

We observe that the only difference between the scheme (3.37)-(3.39) and the scheme (3.21)-(3.23) is that one has to compute an extra explicit term $B_k(|\nabla m^n|^2 m^n)$ in (3.37).

4. Energy decreasing and length preserving schemes for (2.7). The schemes presented in the last section preserve the length constraint $|m| = 1$, but we are unable to show that they are energy decreasing. In fact, we do not aware of any schemes for the Landau-Lifshitz equation (2.9) which are both energy decreasing and length conserving. In this section, we construct schemes which are both energy decreasing schemes and length preserving for Landau-Lifshitz equation (2.9) by introducing an extra Lagrange multiplier $\xi(t)$, which is independent of spatial variables, to enforce energy dissipation. More precisely, we consider the following expanded system for (2.9):

$$(4.1) \quad \begin{aligned} m_t &= \Delta m + \lambda(\mathbf{x}, t)m, \\ m &= \frac{m + \xi(t)}{|m + \xi(t)|}, \\ \frac{d}{dt} E(u) &= - \int_{\Omega} |m \times \Delta m|^2 d\mathbf{x}, \end{aligned}$$

where $E(u) = \frac{1}{2} \int_{\Omega} |\nabla m|^2 d\mathbf{x}$. Note that the Lagrange multiplier $\xi(t)$ is introduced to enforce energy dissipation. Obviously, with $\xi(t) \equiv 0$, the above system reduces to (2.9).

Assuming \tilde{m}^n , m^n and λ^n are known, a Type-I first-order scheme for (4.1) is as follows:

Step 1 (Predictor): solve \tilde{m}^{n+1} from

$$(4.2) \quad \frac{\tilde{m}^{n+1} - m^n}{\delta t} = \Delta \tilde{m}^{n+1} + \lambda^n m^n,$$

Step 2 (Corrector): solve $(\hat{m}^{n+1}, \lambda^{n+1})$ from

$$(4.3) \quad \frac{\hat{m}^{n+1} - \tilde{m}^{n+1}}{\delta t} = \lambda^{n+1} \hat{m}^{n+1} - \lambda^n m^n,$$

$$(4.4) \quad |\hat{m}^{n+1}| = 1,$$

Step 3 (Preserving energy dissipation): solve (m^{n+1}, ξ^{n+1}) from

$$(4.5) \quad m^{n+1} = \frac{\hat{m}^{n+1} + \xi^{n+1}}{|\hat{m}^{n+1} + \xi^{n+1}|},$$

$$(4.6) \quad \frac{E^{n+1} - E^n}{\delta t} = -\|\hat{m}^{n+1} \times \Delta \hat{m}^{n+1}\|^2,$$

where the energy approximation E^{n+1} is defined by

$$(4.7) \quad E^{n+1} = \frac{1}{2} \int_{\Omega} |\nabla m^{n+1}|^2 d\mathbf{x}.$$

Note that the first-two steps (4.2)-(4.4) can be solved the same way as the scheme (3.1)-(3.3). In particular, the consistent solution to the second step is:

$$(4.8) \quad \lambda^{n+1} = \frac{1 - |\tilde{m}^{n+1} - \delta t \lambda^n m^n|}{\delta t}, \quad \hat{m}^{n+1} = \frac{\tilde{m}^{n+1}}{|\tilde{m}^{n+1}|}.$$

It remains to determine ξ^{n+1} and m^{n+1} from the Step 3. Plugging (4.8) into (4.5) and (4.6), we obtain a nonlinear algebraic equation for ξ^{n+1} :

$$(4.9) \quad F(\xi^{n+1}) := E^{n+1} - E^n + \delta t \|\hat{m}^{n+1} \times \Delta \hat{m}^{n+1}\|^2,$$

where E^{n+1} is defined by

$$(4.10) \quad E^{n+1} = \frac{1}{2} \int_{\Omega} |\nabla \frac{\hat{m}^{n+1} + \xi^{n+1}}{|\hat{m}^{n+1} + \xi^{n+1}|}|^2 d\mathbf{x}.$$

To solving the above nonlinear algebraic equation, we can use either the Newton iteration or the following secant method:

$$(4.11) \quad \xi_{k+1} = \xi_k - \frac{F(\xi_k)(\xi_k - \xi_{k-1})}{F(\xi_k) - F(\xi_{k-1})}.$$

Since ξ^{n+1} is an approximation to zero, we can choose $\xi_1 = 0$ and $\xi_0 = -O(\delta t^2)$. In all our experiments, (4.11) converges in a few iterations so that the cost is negligible. Once we obtain ξ^{n+1} , we can update m^{n+1} by (4.5).

Obviously, the scheme (4.2)-(4.6) is first-order accurate, and it is unconditionally energy stable in the sense that of (4.6).

A second-order energy length preserving and energy decreasing scheme based on Crank-Nicolson is as follows:

Step 1 (Predictor): solve \tilde{m}^{n+1} from

$$(4.12) \quad \frac{\tilde{m}^{n+1} - m^n}{\delta t} = \Delta \frac{\tilde{m}^{n+1} + m^n}{2} + \lambda^n m^n,$$

Step 2 (Corrector): solve $(\hat{m}^{n+1}, \lambda^{n+1})$ from

$$(4.13) \quad \frac{\hat{m}^{n+1} - \tilde{m}^{n+1}}{\delta t} = \frac{\lambda^{n+1} \hat{m}^{n+1} - \lambda^n m^n}{2},$$

$$(4.14) \quad |\hat{m}^{n+1}| = 1,$$

Step 3 (Preserving energy dissipation): solve (m^{n+1}, ξ^{n+1}) from

$$(4.15) \quad m^{n+1} = \frac{\hat{m}^{n+1} + \xi^{n+1}}{|\hat{m}^{n+1} + \xi^{n+1}|},$$

$$(4.16) \quad \frac{E^{n+1} - E^n}{\delta t} = -\left\| \frac{\hat{m}^{n+1} + m^n}{2} \times \Delta \frac{\hat{m}^{n+1} + m^n}{2} \right\|^2.$$

Note that the solution procedure for the above scheme is essentially the same as that of (4.2)-(4.6).

Similarly, we can construct Type-II energy decreasing and length conserving schemes for (2.8).

5. Extension to the more general Landau-Lifshitz equation (2.6) with $\beta \neq 0$. In this section, we extend our Lagrange multiplier approach to construct Type-I schemes for the more general Landau-Lifshitz equation (2.6). Similar Type-II schemes can be constructed for (2.3).

If we treat the additional term $\beta m \times \Delta m$ totally explicitly, all the schemes that we constructed in the last two sections for (2.9) can be directly extended to (2.6). Indeed, the Type-I k -th order BDF schemes for (2.6) can be constructed as follows:

Step 1 (Predictor): solve \tilde{m}^{n+1} from

$$(5.1) \quad \frac{\alpha_k \tilde{m}^{n+1} - A_k(m^n)}{\delta t} = \gamma(\Delta \tilde{m}^{n+1} + B_{k-1}(\lambda^n m^n)) - \beta B_{k-1}(m^n \times \Delta m^n),$$

Step 2 (Corrector): solve (m^{n+1}, λ^{n+1}) from

$$(5.2) \quad \frac{\alpha_k(m^{n+1} - \tilde{m}^{n+1})}{\delta t} = \gamma(\lambda^{n+1} m^{n+1} - B_{k-1}(\lambda^n m^n)),$$

$$(5.3) \quad |m^{n+1}| = 1,$$

where α_k , and A_k are defined as before.

However, explicit treatment of $\beta m \times \Delta m$ may lead to a severe time step constraint. Below, we shall construct an efficient length preserving scheme combining a stabilization technique [30] coupled with a Gauss-Seidel approach [32, 22].

We first rewrite (2.6) in the following form

$$(5.4) \quad m_t - S(\Delta m - \Delta m) + \beta m \times \Delta m = \gamma(\Delta m + \lambda(x, t)m),$$

$$|m| = 1,$$

where $S > 0$ is a stabilization constant which will help to stabilize the time discretization.

Similarly to the scheme (3.21)-(3.23), we construct the following Type-I second-order length preserving schemes for (5.4):

Step 1 (Gauss-Seidel predictor): solve $(\tilde{m}_1^{n+1}, \tilde{m}_2^{n+1}, \tilde{m}_3^{n+1})$ from

$$(5.5) \quad \begin{aligned} \frac{\tilde{m}_1^{n+1} - m_1^n}{\delta t} - (S + \gamma)\Delta \tilde{m}_1^{n+1} &= \gamma \lambda^n m_1^n - \beta(\tilde{m}_2^{n,\dagger} \Delta \tilde{m}_3^{n,\dagger} - \tilde{m}_3^{n,\dagger} \Delta \tilde{m}_2^{n,\dagger}) - S\Delta \tilde{m}_1^{n,\dagger}, \\ \frac{\tilde{m}_2^{n+1} - m_2^n}{\delta t} - (S + \gamma)\Delta \tilde{m}_2^{n+1} &= \gamma \lambda^n m_2^n + \beta(\tilde{m}_1^{n+\frac{1}{2}} \Delta \tilde{m}_3^{n,\dagger} - \tilde{m}_3^{n,\dagger} \Delta \tilde{m}_1^{n+\frac{1}{2}}) - S\Delta \tilde{m}_2^{n,\dagger}, \\ \frac{\tilde{m}_3^{n+1} - m_3^n}{\delta t} - (S + \gamma)\Delta \tilde{m}_3^{n+1} &= \gamma \lambda^n m_3^n - \beta(\tilde{m}_1^{n+\frac{1}{2}} \Delta \tilde{m}_2^{n+\frac{1}{2}} - \tilde{m}_2^{n+\frac{1}{2}} \Delta \tilde{m}_1^{n+\frac{1}{2}}) - S\Delta \tilde{m}_3^{n,\dagger}, \end{aligned}$$

where $m_k^{n,\dagger} = \frac{3}{2}m_k^n - \frac{1}{2}m_k^{n-1}$ and $\tilde{m}_k^{n+\frac{1}{2}} = \frac{\tilde{m}_k^{n+1} + m_k^n}{2}$ for $k = 1, 2, 3$.

Step 2 (Corrector): solve (m^{n+1}, λ^{n+1}) from

$$(5.6) \quad \frac{m^{n+1} - \tilde{m}^{n+1}}{\delta t} = \gamma \frac{\lambda^{n+1} m^{n+1} - \lambda^n m^n}{2},$$

$$(5.7) \quad |m^{n+1}| = 1.$$

Note that in the Step 1, a Gauss-Seidel approach is used to deal with the term $\beta m \times \Delta m$. It is shown in [32] that the Gauss-Seidel approach for $\beta m \times \Delta m$ can improve the stability compared with the totally explicit treatment while only requiring to solve a sequence of constant coefficient elliptic problems. The solution procedure for the second step is the same as in (3.22)-(3.23).

We can also add an additional step to the above scheme to preserve the energy dissipation as in the last section. For instance, a second-order length-preserving and energy stable scheme for (5.4) can be constructed as follows:

Step 1 (Gauss-Seidel predictor): exactly the same as (5.1).

Step 2 (Corrector): solve $(\hat{m}^{n+1}, \lambda^{n+1})$ from

$$(5.8) \quad \frac{\hat{m}^{n+1} - \tilde{m}^{n+1}}{\delta t} = \gamma \frac{\lambda^{n+1} \hat{m}^{n+1} - \lambda^n m^n}{2},$$

$$(5.9) \quad |\hat{m}^{n+1}| = 1.$$

Step 3 (Preserving energy dissipation): solve (m^{n+1}, ξ^{n+1}) from

$$(5.10) \quad m^{n+1} = \frac{\hat{m}^{n+1} + \xi^{n+1}}{|\hat{m}^{n+1} + \xi^{n+1}|},$$

$$(5.11) \quad \frac{E^{n+1} - E^n}{\delta t} = -\gamma \left\| \frac{\hat{m}^{n+1} + m^n}{2} \times \Delta \frac{\hat{m}^{n+1} + m^n}{2} \right\|^2.$$

Note that the second step is the same as above, so it can be solved in the same way. On the other hand, the last step is exactly the same as in the scheme (4.2)-(4.6).

Remark 5.1. For (5.1), we use a Gauss-Seidel approach which can increase allowable time steps for stable computation, see [32]. We only need to solve three Poisson type equations from (5.1), the computational cost is the same as a usual semi-implicit scheme.

6. Numerical results. In this section, we implement numerical experiments to validate the convergence rate, accuracy, stability for type-I and type-II schemes we constructed above. Numerical results are shown for Landau-Lifshitz equation (1.1). In space we consider periodic boundary condition and use Fourier-Spectral method [29, 9].

6.1. Convergence rate with a known exact solution. We shall test the convergence rate for the general Landau-Lifshitz equation (5.4) with an external force so that the exact solution is

$$(6.1) \quad \begin{aligned} m_1^e(x, y, t) &= \sin(t + x) \cos(t + y), \\ m_2^e(x, y, t) &= \cos(t + x) \cos(t + y), \\ m_3^e(x, y, t) &= \sin(t + y). \end{aligned}$$

We set $\Omega = [0, 2\pi)^2$ with periodic boundary conditions and use the Fourier spectral method with 128×128 modes for spatial approximation so that the spatial discretization error is negligible. To test convergence rates, we calculate the average L^∞ errors which is defined by

$$(6.2) \quad \|m - m^e\|_{L^\infty} = \frac{\|m_1^e - m_1\|_{L^\infty} + \|m_2^e - m_2\|_{L^\infty} + \|m_3^e - m_3\|_{L^\infty}}{3},$$

where $m = (m_1, m_2, m_3)$ and $m^e = (m_1^e, m_2^e, m_3^e)$ are the numerical solution and exact solution.

We observe from Table. 1 that the expected convergence rates are obtained for schemes (5.1)-(5.3) with $k = 1, 2, 3$ where the parameters are chosen to be $\gamma = \beta = 1$ in (5.4). For the case $\gamma = 1$ and $\beta = 0$ in (5.4), the Crank-Nicolson scheme (3.34)-(3.36) also achieves the second order convergence from Table. 1.

δt	BDF1	Order	BDF2	Order	BDF3	Order	CN	Order
1.6×10^{-3}	$3.02E(-5)$	—	$3.89E(-6)$	—	$6.97E(-10)$	—	$2.03E(-6)$	—
8×10^{-4}	$1.51E(-5)$	1.00	$9.72E(-7)$	2.00	$9.09E(-11)$	2.94	$5.06E(-7)$	2.01
4×10^{-4}	$7.89E(-6)$	0.94	$2.43E(-7)$	2.00	$1.20E(-11)$	2.92	$1.26E(-7)$	2.00
2×10^{-4}	$3.95E(-6)$	0.99	$6.07E(-8)$	2.00	$1.53E(-12)$	2.97	$3.15E(-8)$	2.00
1×10^{-4}	$1.97E(-6)$	1.00	$1.51E(-8)$	2.00	$2.18E(-13)$	2.81	$7.87E(-9)$	2.00
5×10^{-5}	$9.86E(-7)$	0.99	$3.79E(-9)$	1.99	$9.70E(-14)$	1.16	$1.96E(-9)$	2.01

TABLE 1

Accuracy test: The average L^∞ error error between $m = (m_1, m_2, m_3)$ and the exact solution m_e at $t = 0.01$ using BDFk schemes for $k = 1, 2, 3$ and Crank-Nicolson scheme (3.34)-(3.36).

6.2. Convergence rate with a unknown exact solution. Next, we test the convergence rate for Crank-Nicolson scheme (3.34)-(3.36), and energy decreasing schemes (4.2)-(4.6) and (4.12)-(4.16) for the special case (2.7) with the initial condition

$$\begin{aligned}
 m_1(x, y, 0) &= \cos(x) \cos(y) \sin(0.1), \\
 m_2(x, y, 0) &= \cos(x) \cos(y) \cos(0.1), \\
 m_3(x, y, 0) &= \sqrt{1 - \cos^2(x) \cos^2(y)},
 \end{aligned}
 \tag{6.3}$$

in the domain $[0, 2\pi]^2$. We also use 128 Fourier modes in each direction for spatial approximation. The exact solution is unknown so we compute a reference solution by fourth-order Runge-Kutta method with a small time step $\delta t = 10^{-6}$. In Table. 2, the average L^∞ errors between numerical solutions and the reference solution are shown. We observe that the Crank-Nicolson scheme (3.34)-(3.36) and the first-order energy decreasing scheme (4.2)-(4.6) achieve second-order and first-order, respectively, while the energy decreasing scheme (4.12)-(4.16) leads to essentially second-order convergence rate but is not as accurate as the Crank-Nicolson scheme (3.34)-(3.36).

δt	CN	Order	(4.2)-(4.6)	order	(4.12)-(4.16)	Order
8×10^{-4}	$1.44E(-3)$	—	$2.22E(-3)$	—	$1.49E(-3)$	—
4×10^{-4}	$1.01E(-5)$	—	$6.14E(-4)$	—	$3.21E(-4)$	2.21
2×10^{-4}	$2.58E(-6)$	1.97	$3.02E(-4)$	1.02	$1.16E(-4)$	1.47
1×10^{-4}	$6.50E(-7)$	1.99	$1.46E(-4)$	1.05	$3.40E(-5)$	1.77
5×10^{-5}	$1.63E(-7)$	1.99	$6.76E(-5)$	1.11	$5.13E(-6)$	2.72
2.5×10^{-5}	$4.12E(-8)$	1.98	$2.97E(-5)$	1.18	$1.26E(-6)$	2.19

TABLE 2

Accuracy test: The average L^∞ error between $m = (m_1, m_2, m_3)$ and the reference solution at $t = 0.01$ using Crank-Nicolson scheme (3.34)-(3.36), energy decreasing scheme (4.2)-(4.6) and (4.12)-(4.16) .

6.3. Comparisons between various second-order schemes. In this subsection, we compare accuracy and stability of various second-order schemes for the special Landau-Lifshitz equation

(2.7). We set $\Omega = [-\frac{1}{2}, \frac{1}{2})^2$, and test the benchmark problem in [4] with the initial condition

$$(6.4) \quad m(\mathbf{x}, 0) = (m_1, m_2, m_3) = \begin{cases} (0, 0, -1)^T & \text{for } |\mathbf{x}| \geq \frac{1}{2}, \\ (\frac{2x_1 A}{A^2 + |\mathbf{x}|^2}, \frac{2x_2 A}{A^2 + |\mathbf{x}|^2}, \frac{A^2 - |\mathbf{x}|^2}{A^2 + |\mathbf{x}|^2})^T & \text{for } |\mathbf{x}| \leq \frac{1}{2}, \end{cases}$$

where $A = (1 - 2|\mathbf{x}|)^4$.

We consider the following second-order schemes:

- The usual second-order semi-implicit scheme

$$(6.5) \quad \frac{m^{n+1} - m^n}{\delta t} = \Delta \frac{m^{n+1} + m^n}{2} + \frac{3}{2} |\nabla m^n|^2 m^n - \frac{1}{2} |\nabla m^{n-1}|^2 m^{n-1}.$$

- The second-order scheme in [33]:

$$(6.6) \quad \begin{aligned} \frac{\tilde{m}^{n+1} - m^n}{\delta t} &= \Delta \frac{\tilde{m}^{n+1} + m^n}{2} + \delta t \nabla (|\nabla m^n|^2) \nabla m^n; \\ m^{n+1} &= \frac{\tilde{m}^{n+1}}{|\tilde{m}^{n+1}|}. \end{aligned}$$

- Type-I Crank-Nicolson predictor-corrector scheme:

$$(6.7) \quad \begin{aligned} \frac{\tilde{m}^{n+1} - m^n}{\delta t} &= \Delta \frac{\tilde{m}^{n+1} + m^n}{2} + \lambda^n m^n; \\ \frac{m^{n+1} - \tilde{m}^{n+1}}{\delta t} &= \frac{\lambda^{n+1} m^{n+1} - \lambda^n m^n}{2}; \\ |m^{n+1}| &= 1. \end{aligned}$$

- Type-II Crank-Nicolson predictor-corrector scheme:

$$(6.8) \quad \begin{aligned} \frac{\tilde{m}^{n+1} - m^n}{\delta t} &= \Delta \frac{\tilde{m}^{n+1} + m^n}{2} + \frac{3}{2} |\nabla m^n|^2 m^n - \frac{1}{2} |\nabla m^{n-1}|^2 m^{n-1} + \lambda^n m^n; \\ \frac{m^{n+1} - \tilde{m}^{n+1}}{\delta t} &= \frac{\lambda^{n+1} m^{n+1} - \lambda^n m^n}{2}; \\ |m^{n+1}| &= 1. \end{aligned}$$

- Type-II BDF2 predictor-corrector scheme:

$$(6.9) \quad \begin{aligned} \frac{3\tilde{m}^{n+1} - 4m^n + m^{n-1}}{2\delta t} &= \Delta \tilde{m}^{n+1} + |\nabla m^{\dagger, n}|^2 m^{n, \dagger} + \lambda^n m^n; \\ \frac{3m^{n+1} - 3\tilde{m}^{n+1}}{2\delta t} &= \lambda^{n+1} m^{n+1} - \lambda^n m^n; \\ |m^{n+1}| &= 1, \end{aligned}$$

where $m^{\dagger, n} = 2m^n - m^{n-1}$.

To compare accuracy of these schemes, we obtain a reference solution by using the fourth-order Runge-Kutta method with a very small time step $\delta t = 10^{-6}$ in time and 64^2 Fourier modes in space. Table. 3 shows the L^∞ error for different schemes with $\delta t = 10^{-4}$. We observe that the simple semi-discrete scheme (6.5) without length preserving is unstable, and Schemes (6.7), (6.8) and (6.9) achieve similar second-order accuracy and the results are much better than that of Scheme (6.6).

T	Scheme-(6.5)	Scheme-(6.6)	Scheme-(6.7)	Scheme-(6.8)	Scheme-(6.9)
0.01	$3.8198E(-07)$	$2.0663E(-06)$	$3.3198E(-09)$	$9.3788E(-08)$	$7.8620E(-07)$
0.02	$1.7265E(-04)$	$6.4858E(-06)$	$3.9061E(-09)$	$6.1995E(-08)$	$2.3073E(-07)$
0.04	NaN	$1.6174E(-05)$	$7.6123E(-09)$	$3.3997E(-08)$	$4.9371E(-08)$
0.06	-	$2.8101E(-05)$	$4.0602E(-08)$	$6.1291E(-08)$	$1.7317E(-08)$
0.08	-	$4.8164E(-05)$	$1.7553E(-07)$	$1.9378E(-07)$	$9.2875E(-09)$
0.10	-	$7.8866E(-05)$	$5.7183E(-07)$	$5.8832E(-07)$	$1.3193E(-08)$
0.12	-	$1.2487E(-04)$	$1.4952E(-06)$	$1.5104E(-06)$	$1.0365E(-07)$
0.16	-	$3.1270E(-04)$	$7.3706E(-06)$	$7.3549E(-06)$	$3.6430E(-06)$

TABLE 3
Comparison of Schemes (6.5)-(6.9).

6.4. Comparison between Type-I and Type-II schemes. In this subsection, we compare the stability and accuracy between Type-I scheme (6.7) and Type-II scheme (6.8) for Landau-Lifshitz equation (2.7) with the initial condition given by (6.4) in the domain $[-\frac{1}{2}, \frac{1}{2}]^2$. We also use Fourier-Spectral method in space with $N = 64$ Fourier modes in each direction.

In Fig. 1, we depict energy curves for numerical solutions computed by Scheme (6.7) and Scheme (6.8) with different time steps. In Fig. 1.(a), we observe that both schemes are stable and can simulate accurate dynamics of Landau-Lifshitz equation (2.7) with time steps $\delta t = 10^{-4}, 10^{-5}$. In Fig. 1.(b) and Fig. 1.(c), it is observed that the Type-II scheme (6.8) can produce more accurate energy curve than the Type-I scheme (6.7) at the larger time step $\delta t = 10^{-3}$. Numerical solutions m at $t = 0, 0.01, 0.2, 0.4, 0.5, 0.8$ projected on xy -plane computed by the type-II Crank-Nicolson scheme are shown in Fig. 2.

6.5. Adaptive time stepping schemes. A main advantage of unconditionally energy stable schemes is that one can adaptively choose time steps based on the accuracy only. Below, we present an adaptive algorithm which can be used with the unconditionally energy stable schemes introduced in previous section.

Algorithm for adaptive time stepping:

Given Solutions at time steps n and $n - 1$; parameters tol , and the preassigned minimum and maximum allowable time steps δt_{min} and δt_{max} .

Step 1 Compute \hat{m}^{n+1} by Crank-Nicolson scheme (4.12)-(4.14) with δt_n .

Step 2 Compute (ξ^{n+1}, m^{n+1}) from (4.15)-(4.16).

Step 3 if $e^{n+1} = |\xi^{n+1}| > tol$, **then**

Recalculate time step $\delta t_n \leftarrow \max\{\delta t_{min}, \min\{A_{dp}(e^{n+1}, \delta t^n), \delta t_{max}\}\}$.

Step 4 **goto** Step 1

Step 5 **else**

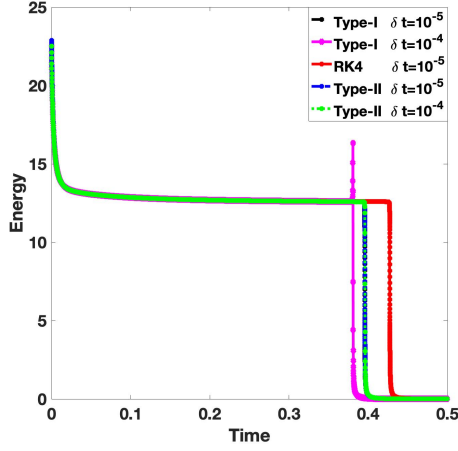
Update time step $\delta t_{n+1} \leftarrow \max\{\delta t_{min}, \min\{A_{dp}(e^{n+1}, \delta t^n), \delta t_{max}\}\}$,

Step 6 **endif**

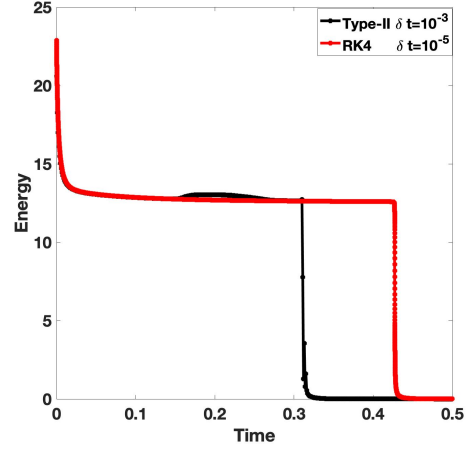
One simple but effective strategy is to update the time step size by using the formula [11],

$$(6.10) \quad A_{dp}(e, \delta t) = \rho \left(\frac{tol}{e} \right)^{\frac{1}{2}} \delta t.$$

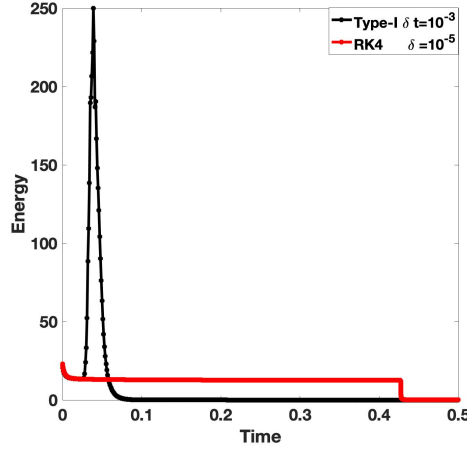
We choose the constant $\rho = 0.95$ for numerical simulations in this subsection. We implemented the above adaptive stepping based on the energy decreasing scheme (4.12)-(4.16) for (2.7) and the energy decreasing scheme (5.8)-(5.11) for (1.1).



(a) Scheme (6.7) and (6.8) with $\delta t = 10^{-4}, 10^{-5}$



(b) Type-II Scheme-(6.8) with $\delta t = 10^{-3}$



(c) Type-I Scheme-(6.7) with $\delta t = 10^{-3}$

FIG. 1. Energy comparison for Crank-Nicolson type-I prediction-correction (6.7) and type-II prediction-correction scheme (6.8) using various time steps.

First, we consider the general Landau-Lifshitz equation (1.1) with the same initial condition (6.4) in the domain $\Omega = [0, 2\pi)^2$ with periodic boundary conditions. The Fourier spectral method is used in space with 128 Fourier modes in each direction. We compute the numerical solution using energy decreasing scheme (4.12)-(4.16) with time step $\delta t = 10^{-4}$. From Fig. 3.(a), we observe that ξ^{n+1} in (4.15)-(4.16) is very close to zero at most of the time and deviates from zero slightly when the energy gradient is large. The evolution of energy computed by energy decreasing scheme (4.12)-(4.16) and its adaptive time stepping scheme are almost the same from Fig. 3.(b). We plot in Fig. 3.(c) the number of iteration needed to solve the nonlinear algebraic equation (4.16) at each time step, and observe that only a few iterations are needed which indicates that the computational cost of energy decreasing scheme (4.12)-(4.16) is comparable with a usual linear semi-implicit scheme.

In the second example, we test the accuracy of the adaptive time stepping scheme based on

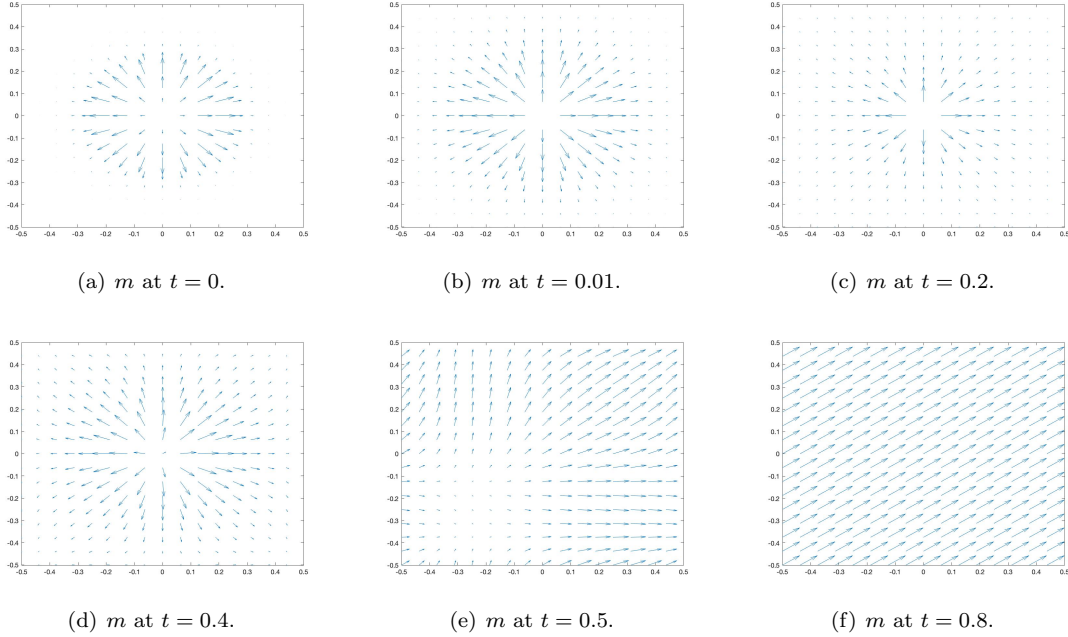


FIG. 2. (a)-(f): Numerical solutions m at $t = 0, 0.01, 0.2, 0.4, 0.5, 0.8$ projected on xy -plane using the type-II Crank-Nicolson scheme with $\delta t = 10^{-4}$.

(4.12)-(4.16). We consider again the benchmark problem for the special Landau-Lifshitz equation (2.7) in Subsection 6.3. The results computed by scheme (4.12)-(4.16) with adaptive time steps are depicted in Fig. 4. We observe first that the profile of energy curve in Fig. 4.(c) is close to energy curve computed by fourth-order Runge-Kutta (RK4) scheme with small time step $\delta t = 10^{-5}$ which indicates that we can obtain accurate numerical solutions using adaptive time stepping method. From Fig. 4.(d), we also observe that only a few iterations are needed at each time step to solve the nonlinear algebraic equation (4.14) using the secant method. We observe from the evolution of time steps in Fig. 4.(b) that the adaptive time stepping method can significantly improve the computational efficiency.

In the third example, we solve the Landau-Lifshitz equation (1.1) with $\beta = \gamma = 1$ in the domain $[-\frac{1}{2}, \frac{1}{2}]^2$ using the adaptive time stepping scheme with tolerance $|\xi| \leq \text{tol} = 5 \times 10^{-5}$ based on (5.8)-(5.11) and 64^2 Fourier modes in space. The initial condition is also chosen to be (6.4). We observe from Fig. 5 that larger time steps can be used when the energy curve change slowly, and the computed energy decreases with time.

6.6. phenomenon of blowup. In this subsection, we investigate the possible blowup of the general Landau-Lifshitz equation (1.1) with certain smooth initial condition which has been studied in [8, 4]. We set $\Omega = [-\frac{1}{2}, \frac{1}{2}]^2, \beta = \gamma = 1$ with the same initial condition as in (6.4). We choose periodic boundary condition in space and implement Fourier spectral method for spatial discretization with Fourier modes $N = 64$ in each direction. Numerical simulations are computed by Gauss-Seidel scheme (5.5)-(5.7) with $\delta t = 10^{-5}$. Displayed in Fig. 6 are the orthogonal projection of the vector field m on the plane $\{(x, y, 0) : x, y \in \mathbb{R}\}$ at various times. We observe that m changes rapidly near origin, indicating that ∇m becomes very large and may blowup. It is observed from Fig. 7 that the spin m at the origin even change from $(0, 0, 1)$ to $(0, 0, -1)$ at $t \approx 0.4$. In Fig. 8.(b), we plot the evolution of $\|\nabla m\|_\infty$ with respect to time, which is consistent with the phenomenon of blowup presented in [8].

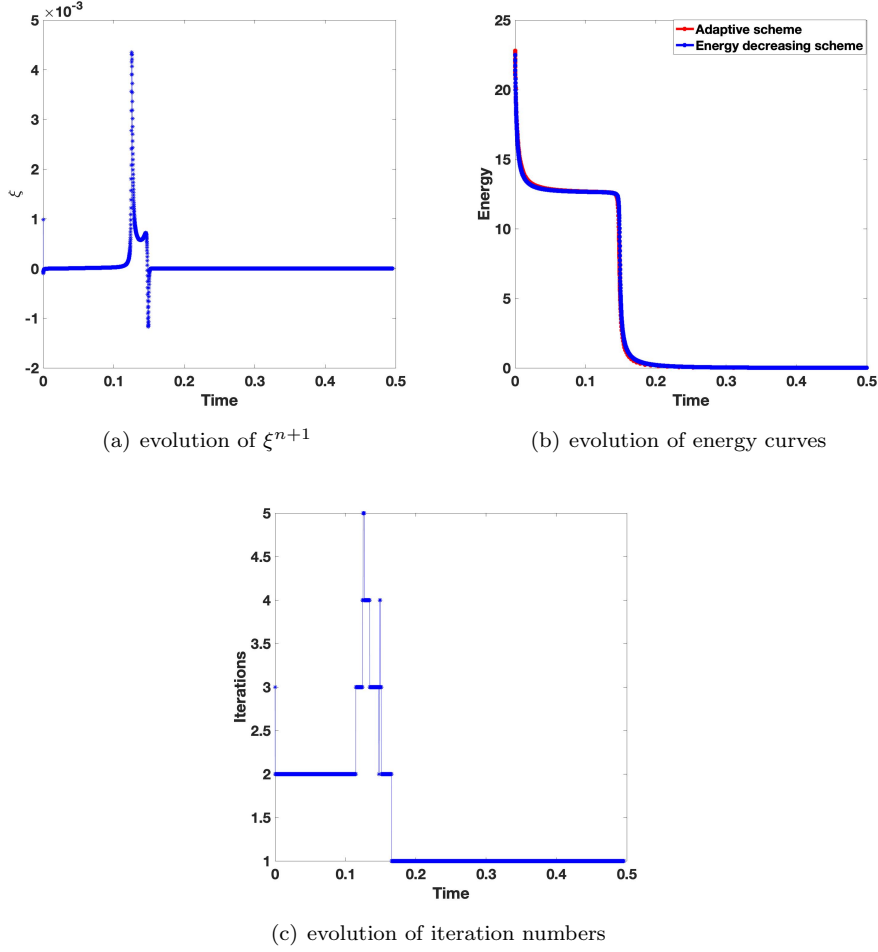


FIG. 3. The evolution of ξ , energy curve and iteration numbers for Landau-Lifshitz equation (2.7) computed by (4.12)-(4.16) with various time step $\delta t = 10^{-4}$.

Using the same initial condition and resolution as above, we also plot in Fig. 8.(b) energy curves computed by the fourth-order Runge-Kutta scheme with $\delta t = 10^{-5}$ and the stabilized type-II Gauss-Seidel scheme with $S = 0.5$ for the general Landau-Lifshitz equation using a larger time step $\delta t = 10^{-2}$. We observe from Fig. 8.(a) that the two energy curves are close to each other which indicates that the stabilization allows us to use much larger time steps for the simulation of the general Landau-Lifshitz equation (1.1).

7. Concluding remarks. We developed in this paper two classes of length preserving, and energy dissipative time discretization schemes for the Landau-Lifshitz equation based on the Lagrange multiplier approach. These schemes are not restricted to any particular spatial discretization, and at each time, the computational cost is dominated by the cost of the predictor step which requires solving decoupled linear elliptic equations with constant coefficients. So the computational costs of these schemes are comparable to a usual semi-implicit scheme, but with the advantage of being length preserving, and can also be energy dissipative. To the best of our knowledge, our schemes based on the predictor-corrector approach are the first length preserving higher than second-order schemes for the Landau-Lifshitz equation, and our schemes with an additional space-

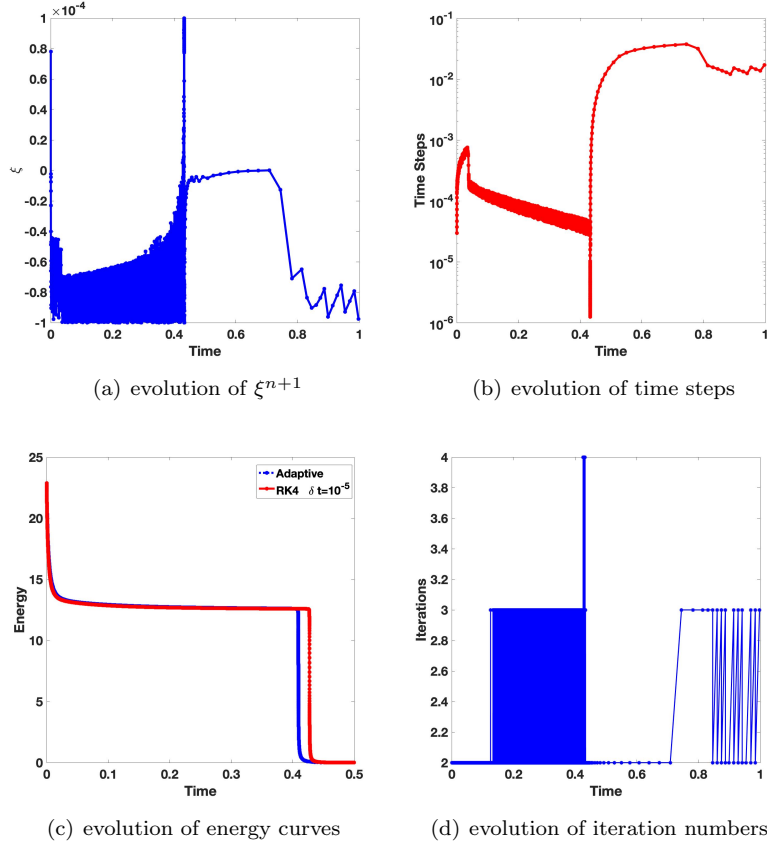


FIG. 4. The evolution of ξ , energy curve and iteration numbers for Landau-Lifshitz equation computed by (4.12)-(4.16) with adaptive time stepping method.

independent Lagrange multiplier are the first length preserving and energy dissipative schemes for the Landau-Lifshitz equation.

We carried out ample numerical experiments to validate the stability and accuracy for the proposed schemes, and also compared them with some existing schemes. It is observed that our predictor-corrector schemes can provide better accuracy than schemes based on projection. We also observed that the Type-II schemes, which are based on a Lagrange multiplier $\lambda = 0$ at the continuous level, usually produce more accurate dynamical approximation than the type-I schemes, which are based on the Lagrange multiplier formulation with $\lambda = |\nabla m|^2$. It is also found that for the general Landau-Lifshitz equation, adding a stabilized term can significantly increase the stability for both type-I and type-II schemes.

The general ideas introduced in this paper for constructing length preserving and energy dissipative schemes are not limited to Landau-Lifshitz equation, and can be applied to other length preserving nonlinear dissipative systems, such as the liquid crystal flows [24, 25]. In this sense, this paper can also be regarded as Part III of the sequence following [12, 13].

We only provided some stability analysis for the simplest first-order scheme in the semi-discrete form. It appears very difficult to establish unconditional stability results for the higher-order schemes in the semi-discrete form. In a future work, we shall consider a fully discretized version of our schemes presented here, and attempt to establish its stability and convergence results with the help of some reasonable conditions on the time step, similar to those in [4, 17].

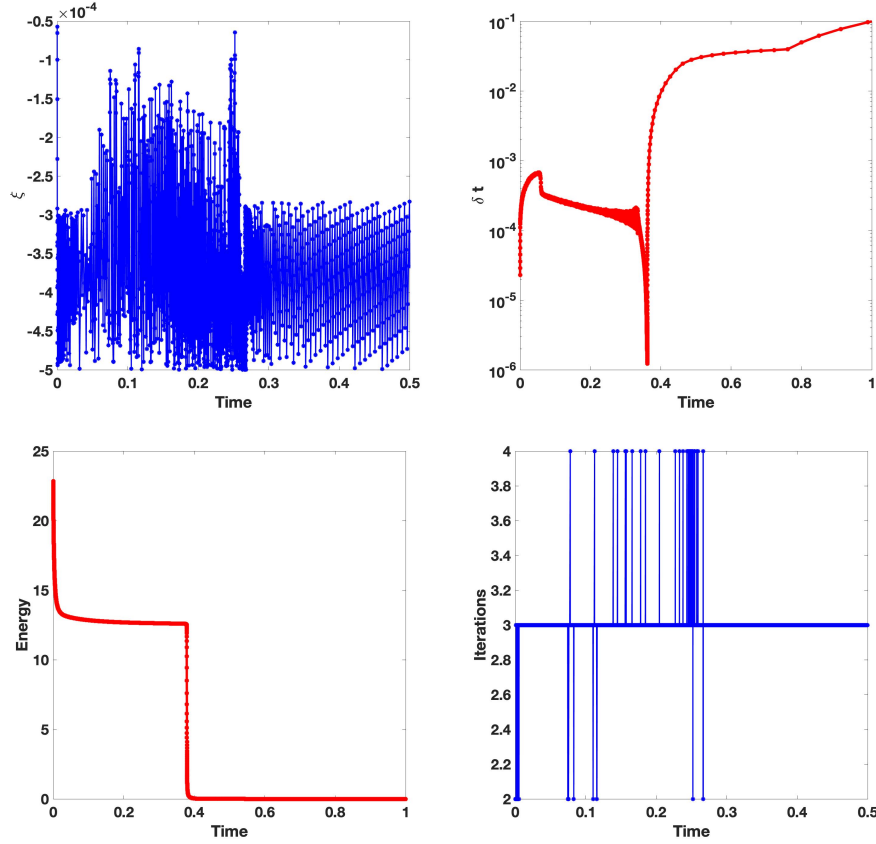


FIG. 5. The evolution of ξ , energy curve and iteration numbers for the general Landau-Lifshitz equation computed by (5.8)-(5.11) with adaptive time stepping method.

REFERENCES

- [1] Georgios Akrivis. Stability of implicit-explicit backward difference formulas for nonlinear parabolic equations. *SIAM Journal on Numerical Analysis*, 53(1):464–484, 2015.
- [2] Georgios Akrivis, Michael Feischl, Balázs Kovács, and Christian Lubich. Higher-order linearly implicit full discretization of the Landau–Lifshitz–Gilbert equation. *Mathematics of Computation*, 90(329):995–1038, 2021.
- [3] François Alouges and Pascal Jaisson. Convergence of a finite element discretization for the Landau–Lifshitz equations in micromagnetism. *Mathematical Models and Methods in Applied Sciences*, 16(02):299–316, 2006.
- [4] Rong An, Huadong Gao, and Weiwei Sun. Optimal error analysis of Euler and Crank–Nicolson projection finite difference schemes for Landau–Lifshitz equation. *SIAM Journal on Numerical Analysis*, 59(3):1639–1662, 2021.
- [5] Rong An and Weiwei Sun. Analysis of backward Euler projection fem for the Landau–Lifshitz equation. *IMA Journal of Numerical Analysis*, 2021.
- [6] Santiago Badia, Francisco Guillén-González, and Juan Vicente Gutiérrez-Santacreu. Finite element approximation of nematic liquid crystal flows using a saddle-point structure. *Journal of Computational Physics*, 230(4):1686–1706, 2011.
- [7] Santiago Badia, Francisco Guillén-González, and Juan Vicente Gutiérrez-Santacreu. An overview on numerical analyses of nematic liquid crystal flows. *Archives of Computational Methods in Engineering*, 18(3):285–313, 2011.
- [8] Sören Bartels, Joy Ko, and Andreas Prohl. Numerical analysis of an explicit approximation scheme for the Landau-Lifshitz-Gilbert equation. *Mathematics of Computation*, 77(262):773–788, 2008.
- [9] Claudio Canuto, M Yousuff Hussaini, Alfio Quarteroni, A Thomas Jr, et al. *Spectral methods in fluid dynamics*.

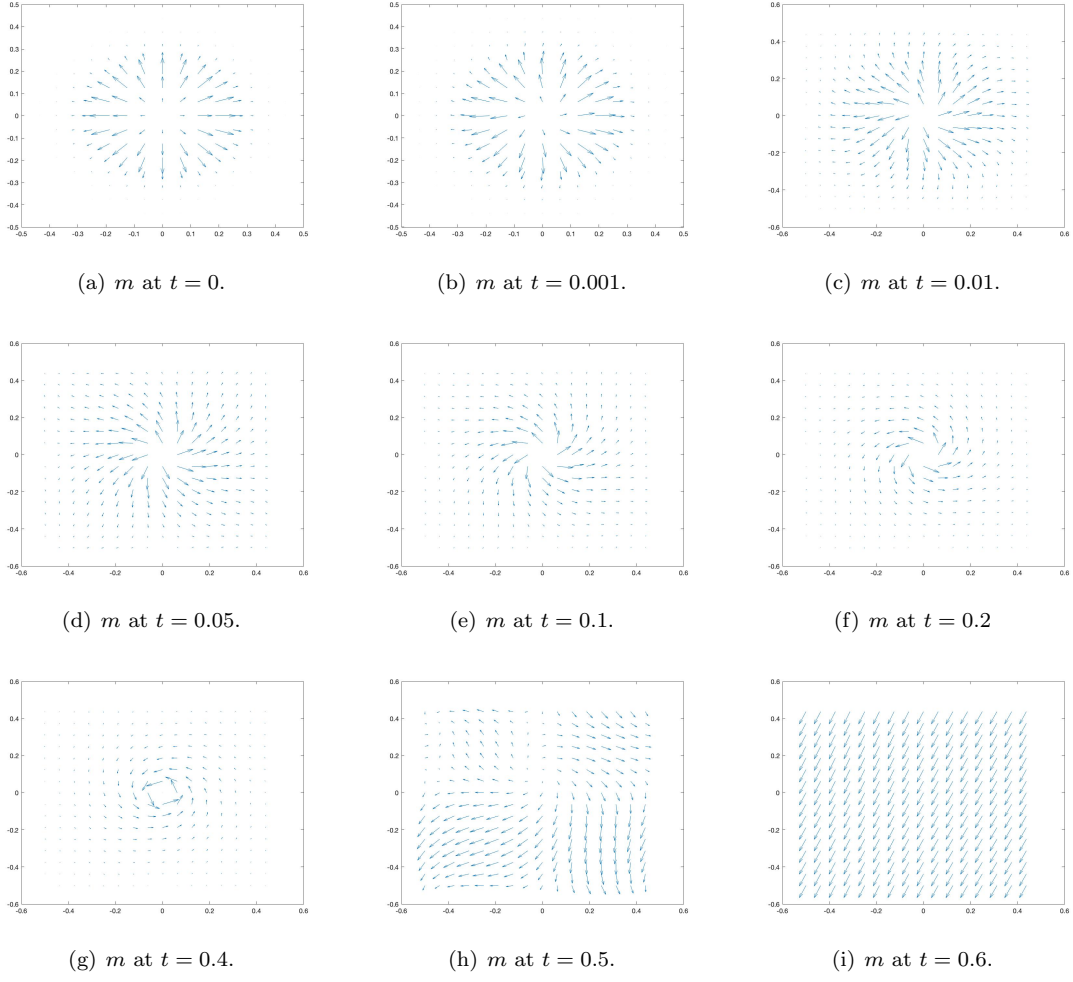


FIG. 6. (a)-(i): Numerical solutions m at $t = 0, 0.001, 0.01, 0.05, 0.1, 0.2, 0.4, 0.5, 0.6$ projected on xy -plane using the second-order Gauss-Seidel predictor-correction scheme (5.5)-(5.7) with $\delta t = 10^{-5}$.

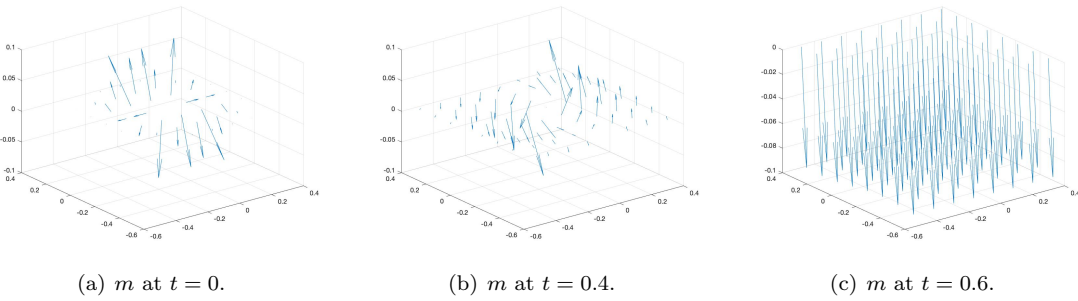


FIG. 7. (a)-(c): Numerical solutions m at $t = 0, 0.4, 0.6$ using the second-order Gauss-Seidel predictor-correction scheme (5.5)-(5.7) with $\delta t = 10^{-5}$.

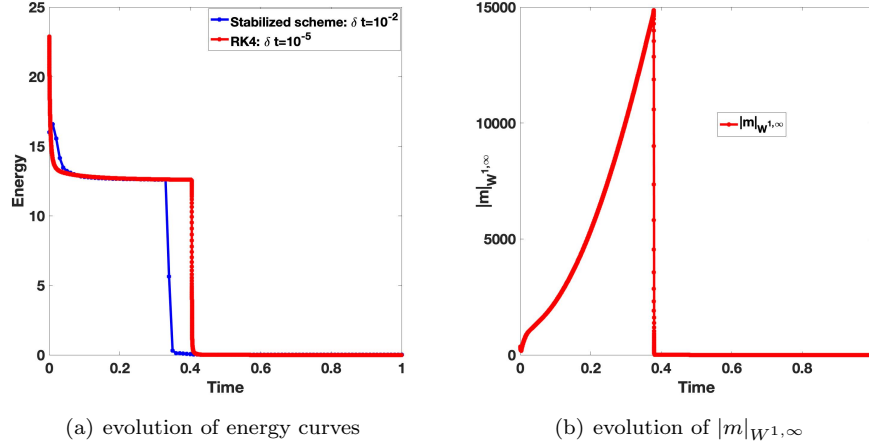


FIG. 8. (a). Comparison of energy curves using stabilized type-II Gauss-Seidel scheme with stabilized constant $S = 0.5$. (b). The evolution of $\|m\|_{W^{1,\infty}}$ for the general Landau-Lifshitz equation computed by Gauss-Seidel (5.5)-(5.7) with time step $\delta t = 10^{-5}$.

- Springer Science & Business Media, 2012.
- [10] Jingrun Chen, Cheng Wang, and Changjian Xie. Convergence analysis of a second-order semi-implicit projection method for Landau-Lifshitz equation. *Applied Numerical Mathematics*, 168:55–74, 2021.
 - [11] Qing Cheng and Jie Shen. Multiple scalar auxiliary variable (MSAV) approach and its application to the phase-field vesicle membrane model. *SIAM Journal on Scientific Computing*, 40(6):A3982–A4006, 2018.
 - [12] Qing Cheng and Jie Shen. A new lagrange multiplier approach for constructing structure preserving schemes, I. positivity preserving. *Computer Methods in Applied Mechanics and Engineering*, 391:114585, 2022.
 - [13] Qing Cheng and Jie Shen. A new lagrange multiplier approach for constructing structure preserving schemes, II. bound preserving. *SIAM Journal on Numerical Analysis*, 60(3):970–998, 2022.
 - [14] A. J. Chorin. Numerical solution of the Navier-Stokes equations. *Math. Comp.*, 22:745–762, 1968.
 - [15] Huadong Gao. Optimal error estimates of a linearized backward Euler FEM for the Landau-Lifshitz equation. *SIAM Journal on Numerical Analysis*, 52(5):2574–2593, 2014.
 - [16] Jean-Luc Guermond, Peter Mineev, and Jie Shen. An overview of projection methods for incompressible flows. *Computer Methods in Applied Mechanics and Engineering*, 195(44-47):6011–6045, 2006.
 - [17] Xinping Gui, Buyang Li, and Jilu Wang. Convergence of renormalized finite element methods for heat flow of harmonic maps. *SIAM Journal on Numerical Analysis*, 60(1):312–338, 2022.
 - [18] Bo Ling Guo and Min Chun Hong. The Landau-Lifshitz equation of the ferromagnetic spin chain and harmonic maps. *Calc. Var. Partial Differential Equations*, 1(3):311–334, 1993.
 - [19] Martin Kruzik and Andreas Prohl. Recent developments in the modeling, analysis, and numerics of ferromagnetism. *SIAM Review*, 48(3):439–483, 2006.
 - [20] M Lakshmanan and K Nakamura. Landau-Lifshitz equation of ferromagnetism: Exact treatment of the gilbert damping. *Physical Review Letters*, 53(26):2497, 1984.
 - [21] Lale Landau and Evgeny Lifshitz. On the theory of the dispersion of magnetic permeability in ferromagnetic bodies. In *Perspectives in Theoretical Physics*, pages 51–65. Elsevier, 1992.
 - [22] Panchi Li, Changjian Xie, Rui Du, Jingrun Chen, and Xiao-Ping Wang. Two improved Gauss-Seidel projection methods for Landau-Lifshitz-Gilbert equation. *Journal of Computational Physics*, 401:109046, 2020.
 - [23] Fanghua Lin and Changyou Wang. *The analysis of harmonic maps and their heat flows*. World Scientific, 2008.
 - [24] Chun Liu and Noel J Walkington. Approximation of liquid crystal flows. *SIAM Journal on Numerical Analysis*, 37(3):725–741, 2000.
 - [25] Chun Liu and Noel J Walkington. Mixed methods for the approximation of liquid crystal flows. *ESAIM: Mathematical Modelling and Numerical Analysis*, 36(2):205–222, 2002.
 - [26] F Pistella and V Valente. Numerical stability of a discrete model in the dynamics of ferromagnetic bodies. *Numerical Methods for Partial Differential Equations: An International Journal*, 15(5):544–557, 1999.
 - [27] Andreas Prohl et al. *Computational micromagnetism*. Springer, 2001.
 - [28] Jie Shen. Long time stability and convergence for fully discrete nonlinear Galerkin methods. *Appl. Anal.*, 38(4):201–229, 1990.
 - [29] Jie Shen, Tao Tang, and Li-Lian Wang. *Spectral methods: algorithms, analysis and applications*, volume 41.

- Springer Science & Business Media, 2011.
- [30] Jie Shen and Xiaofeng Yang. Numerical approximations of Allen-Cahn and Cahn-Hilliard equations. *Discrete & Continuous Dynamical Systems*, 28(4):1669, 2010.
 - [31] Roger Temam. Une méthode d’approximation de la solution des équations de navier-stokes. *Bulletin de la Société Mathématique de France*, 96:115–152, 1968.
 - [32] Xiao-Ping Wang, Carlos J Garcia-Cervera, and E Weinan. A Gauss–Seidel projection method for micromagnetics simulations. *Journal of Computational Physics*, 171(1):357–372, 2001.
 - [33] E Weinan and Xiao-Ping Wang. Numerical methods for the Landau-Lifshitz equation. *SIAM Journal on Numerical Analysis*, pages 1647–1665, 2001.